XXI IMEKO World Congress "Measurement in Research and Industry"
August 30 – September 4, 2015, Prague, Czech Republic

UNCERTAINTY ESTIMATION OF SHOCK TUBE PRESSURE STEPS

Stephen Downes [1], *Andy Knott* [2], *and Ian Robinson* [3]

[1] National Physical Laboratory, Teddington, United Kingdom, stephen.downes@npl.co.uk
[2] National Physical Laboratory, Teddington, United Kingdom, andy.knott@npl.co.uk
[3] National Physical Laboratory, Teddington, United Kingdom, ian.robinson@npl.co.uk

Abstract – In this paper we describe the work performed at the National Physical Laboratory (NPL) to develop dynamic pressure standards based on shock tube techniques, including the checks carried out to ensure that the ideal gas theory, used to predict step pressure changes, is valid in our circumstances. We go on to consider the major uncertainty contributions to the calculated step pressure, suggest ways to minimise these, and conclude by calculating a target uncertainty for NPL's new 7.0 MPa steel shock tube.

Keywords: shock tube, dynamic pressure, uncertainty

1. INTRODUCTION

As part of a project to develop dynamic pressure standards for industrial traceability, NPL has developed a shock tube system based on plastic tubing capable of generating step pressures of up to 1.4 MPa [1]. This cheap and easily modifiable system has been used to investigate the feasibility of dynamically calibrating pressure transducers using a shock tube. The knowledge and experience gained during this work have informed the design of a 7.0 MPa steel shock tube, currently under construction.

2. INDUSTRIAL REQUIREMENTS

Many industrial pressure measurements are made while the pressure is rapidly changing. The transducers used to make these measurements are, in general, only calibrated statically, due to the lack of dynamic calibration facilities. The assumption is made that the statically-determined sensitivity is valid under the dynamic conditions experienced in the measurement applications. In some of the more demanding of these applications, such as in-cylinder pressure measurement for automotive engine development, an uncertainty in pressure measurement of better than 1 % at frequencies of up to 30 kHz would offer engine developers significant support in their efforts to maximise fuel efficiency and minimise NO_x emissions.

To establish dynamic pressure calibration facilities, a method of generating a known dynamic pressure, traceable to the SI, must be employed [2]. One of the only methods available for giving traceability at these high frequencies employs the extremely fast and calculable pressure step generated across a shock front in a shock tube.

3. SHOCK TUBE THEORY

A shock tube consists of two gas-filled sections; a high pressure driver section and a lower pressure driven section, initially separated by a diaphragm. The pressure in the driver section is increased slowly until the diaphragm ruptures, and a shock front propagates through the driven gas. Fig. 1 illustrates chronologically the stages of operation, with Fig. 1.a showing the condition of the tube at the moment that the diaphragm bursts. The driver section is at a uniform pressure p_4 and the driven section is at a uniform pressure p_1. In Fig. 1.b the shock front is propagating into the driven gas with a constant pressure p_2 behind it. The contact surface between the driven and driver gases is propagating in the same direction as the shock front but at a lower speed. In Fig. 1.c the rarefaction wave has reflected from the end of the driver section and is propagating towards the other end of the tube. In Fig. 1.d the shock wave has reflected from the end-wall of the tube and the pressure behind it has risen to p_5.

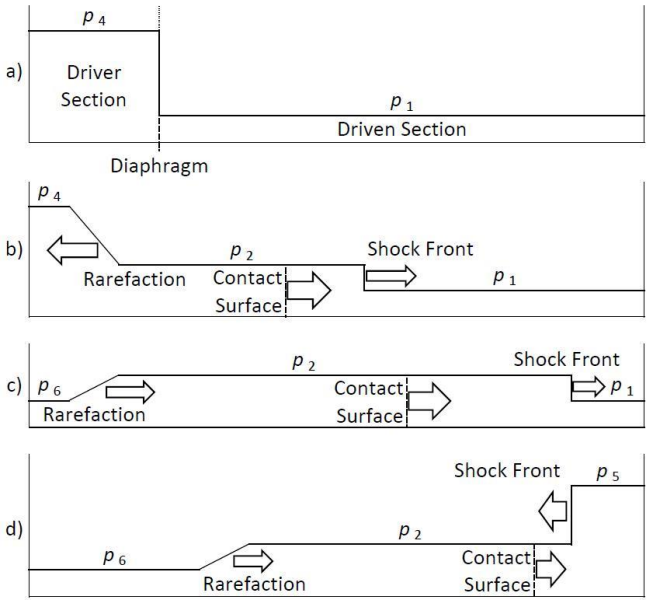

Fig. 1. Shock tube operation (the x-axis represents the tube length and the y-axis gives the pressure in that part of the tube).

At the time of arrival of the shock wave, a sensor in the centre of the end-wall of the tube sees a pressure step Δp of amplitude $p_5 - p_1$, and the measured pressure then remains

stable at p_5 until the arrival of a second shock front, resulting from the initial shock front's partial reflection from the contact surface. The extremely fast rise in pressure (taking a time of the order of 1 ns [3]) to a stable value, associated with the arrival of the initial shock wave, provides the basis for a dynamic calibration of pressure transducers.

Ideal gas theory [4] enables the magnitude of the pressure step Δp to be calculated from (1), in which p_1 is the initial gas pressure in the driven section and $\mathcal{M}$ is the Mach number of the shock wave. The Mach number $\mathcal{M}$ is calculated as v_S/c_1, where v_S is the velocity of the shock front and c_1 is the speed of sound in the undisturbed gas in the driven section; c_1 is given by (2), in which γ is the adiabatic index, R is the molar gas constant, T is the absolute temperature, and M is the average molar mass of the gas.

$$\Delta p = 14 p_1 \left(2\mathcal{M}^4 - \mathcal{M}^2 - 1\right)/\left(3(\mathcal{M}^2 + 5)\right) \qquad (1)$$

$$c_1 = \sqrt{(\gamma RT/M)} \qquad (2)$$

For a gas of known properties in the driven section, the theoretical pressure step can be derived from measurements of its initial temperature and pressure and the velocity of the shock front. The shock velocity measurement is made by recording, on a common time base, the outputs from pressure transducers located set distances apart along the tube wall. As the shock wave passes over each transducer diaphragm, set nominally flush to the inner tube wall, the rise in pressure causes an increase in the transducer output voltage. Fig. 2 shows the outputs from three side-wall transducers set at 200 mm intervals, the shock velocity being calculated from this spacing and the times between the recorded rapid rises in output.

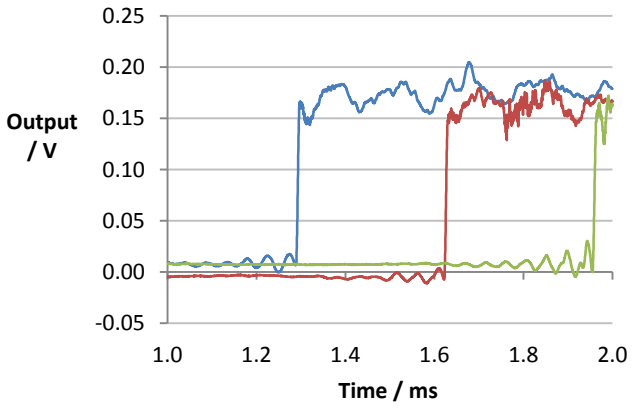

Fig. 2. Side-wall pressure transducer output traces.

4. MODEL VALIDATION

To determine the validity of the theory in a practical apparatus, a number of tests were performed in NPL's 1.4 MPa shock tube. For each test, the same piezoelectric pressure transducer was located in the centre of a steel mount held in the tube's end-wall, with its diaphragm flush to the surface of the mount. The shock velocity was calculated from the side-wall transducer outputs and used, together with the temperature and gas species information, to determine the shock wave's Mach number. This was then combined with the initial driven section pressure p_1 to calculate the theoretical value of Δp for each test. The output from the end-wall transducer was then divided by this pressure step to generate a plot of transducer sensitivity against time – for a linear transducer (one in which the sensitivity does not vary with applied pressure), the plots from the different tests should overlay each other if the theory is correct and applicable. Fig. 3 shows three such traces, derived from tests in which p_1 was varied by partially evacuating the driven section.

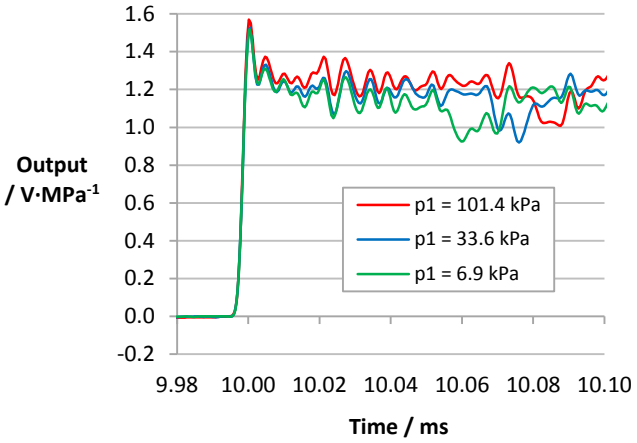

Fig. 3. Effect of variation of initial driven section pressure on transducer response.

Despite an uncertainty of a few percent in the measured value of p_1 at the two lower pressures, leading to a significant uncertainty in the associated calculated pressure steps, there is reasonable agreement between these three traces. Similar checks will be performed in the steel tube using pressure measurement equipment of lower uncertainty.

Fig. 4 shows the results of further tests designed to determine the effects of variations in shock velocity and driven section gas species. In order to facilitate a comparison with the transducer's stated static sensitivity (-47.59 pC·MPa^{-1}), the output voltage traces have been converted back into raw charge traces prior to being divided by the pressure step value.

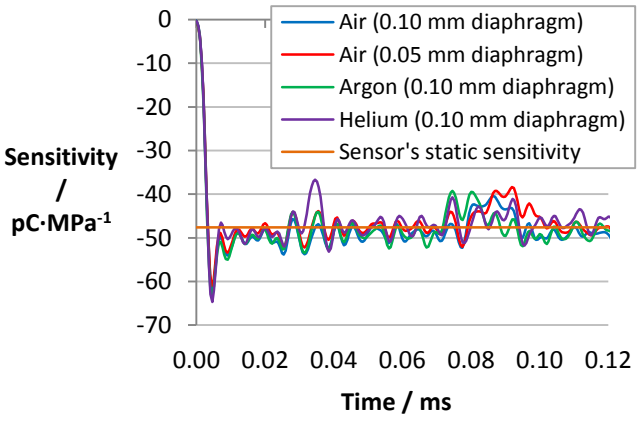

Fig. 4. Effect of variation of shock wave velocity and driven section gas species on transducer response.

Much of the dynamic content in the voltage traces shown in Fig. 3 and Fig. 4 results from the transducer's sensitivity

to vibration [5]. These effects can be significantly reduced by the use of a plastic mounting adaptor but, for consistency, all of these tests were performed without such an adaptor.

5. UNCERTAINTY BUDGET

Values of $u_{\mathcal{M}}$ and $u_{\Delta p}$, the standard uncertainties associated with the calculated Mach speed of the shock front and the pressure step Δp respectively, can be estimated from (3) and (4), in which u_{v_S}, u_{c_1}, and u_{p_1} are the standard uncertainties associated with v_S, c_1, and p_1 respectively.

$$u_{\mathcal{M}} = (1/c_1)\sqrt{u_{v_S}^2 + \mathcal{M}^2 u_{c_1}^2} \quad (3)$$

$$u_{\Delta p} = \sqrt{\left(\frac{\Delta p}{p_1}u_{p_1}\right)^2 + \left(56 p_1 \mathcal{M} u_{\mathcal{M}} \left(\frac{\mathcal{M}^4+10\mathcal{M}^2-2}{3(\mathcal{M}^2+5)^2}\right)\right)^2} \quad (4)$$

From (4), the effect of shock velocity uncertainty u_{v_S} on the uncertainty of the pressure step can be calculated and is plotted in Fig. 5, as a function of Δp, assuming minimal contributions from u_{c_1} and u_{p_1}.

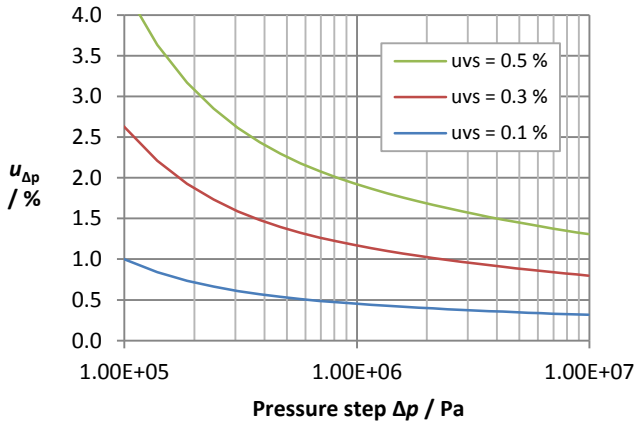

Fig. 5. Effect of shock velocity uncertainty on uncertainty of pressure step.

It is apparent that, in order to achieve a standard uncertainty of better than 0.5 % for the pressure step (to give a $k = 2$ expanded uncertainty lower than 1 %) in the range from 1 MPa to 7 MPa, the standard uncertainty of the shock velocity value needs to be lower than 0.1 %.

6. SHOCK VELOCITY MEASUREMENT

The two components associated with the velocity measurement are the distance between the side-wall transducers and the time the shock wave takes to travel between them. Both of these parameters need to be accurately determined, if the target standard uncertainty of 0.1 % is to be achieved.

6.1. Time measurement

Fig. 6 shows the rising edges of the traces from Fig. 2, with the red and green traces shifted in both x and y directions to overlay the blue trace. The x-direction shift gives the time taken for the shock wave to travel between the two transducer locations.

It is clear that the traces do not overlay perfectly and this is a source of uncertainty. It may be that the underlying transducer or charge amplifier characteristics are slightly different but it seems more likely that the disturbance to the transducer prior to the arrival of the shock front (visible on all three output traces in Fig. 2) affects its performance during the shock front transition. It is assumed that this disturbance is caused by elastic deformation of the tube ahead of the shock front and hoped that this effect will be less apparent in the steel shock tube. For the plastic tube, a standard uncertainty on the time interval of 0.5 µs is taken as a reasonable estimate. For a shock travelling at 556 m·s^{-1} (Mach number 1.62) between transducers 400 mm apart, this interval corresponds to a standard uncertainty of 0.07 % of the measured time.

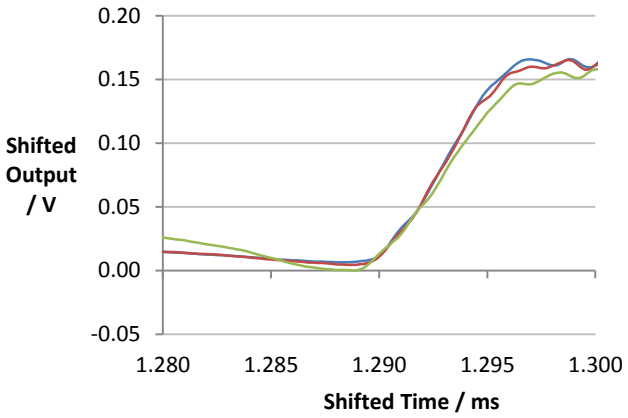

Fig. 6. Time-shifted rising edges of side-wall transducer traces.

6.2. Distance measurement

The holes for the sensors in the plastic tube were drilled by hand using pre-drilled holes in an aluminium block clamped to the tube surface. Although the separation between the pre-drilled holes is (200.0 ± 0.1) mm, the standard uncertainty on the distance between the ends of successive pairs of holes in the tube wall is estimated to be 0.25 mm. For the steel tube, the actual dimensions will be measured on a coordinate measuring machine, giving a greatly-reduced uncertainty.

The assumption that a pressure transducer output shows the greatest rate of change as the shock front crosses the centre of the diaphragm was tested by recording the output from two transducers set next to each other on the same tube circumferential section. The time between the shock front passing the two diaphragms was estimated and then the test was repeated. One transducer was then rotated through 90° while leaving the other one alone, and the test carried out twice more. This process was repeated three times, to give ten test results in total, showing shock arrival time separation as a function of one transducer's orientation. These results are plotted in Fig. 7 together with a best-fit sinusoid.

The results indicate that, in the plastic tube, the rotated transducer's time of response appears to be sensitive to its orientation, suggesting that its point of maximum response is not at its geometric centre. This conclusion is based on the assumption that the transducer's sliding fit in the hole ensures a repeatable diaphragm location throughout its rotation. The 1.1 µs peak-to-peak spread at a shock wave

velocity of 590 m·s^{-1} is equivalent to a distance of 0.65 mm. This corresponds to a distance of 0.32 mm between the centre of the diaphragm and its point of maximum response.

The steel tube has been designed to enable this parameter to be measured against a reference pressure transducer. The results of these checks will enable the transducers to be oriented so as to place the point of maximum response and the geometric centre on a common circumference of the tube, nulling the effect.

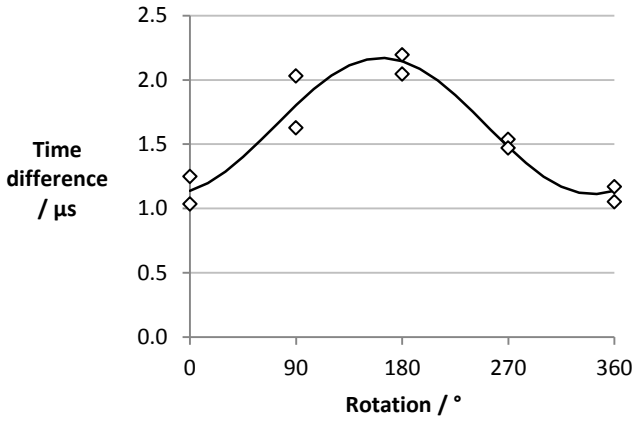

Fig. 7. Shock arrival time difference as a function of orientation.

6.3. Discussion

To minimise the relative uncertainty contributions arising from measurements of length and time, it would make sense to situate the side-wall transducers a long way apart. However, the velocity of interest is that of the shock front as it reaches the end-wall while the measured velocity is the average value between the two transducer locations. If it can be shown, by using three side-wall transducers, that the shock front moves at constant speed, as theory suggests, a large transducer separation would be the best approach. If it is shown that the shock front is either accelerating or decelerating, the velocity at the end-wall will need to be extrapolated from velocity measurements along the tube, and making measurements near the end of the tube with closely spaced transducers may also prove necessary.

The 2 m-long steel shock tube will have one side-wall transducer located near the end-wall, and three further possible transducer locations at distances of 200 mm, 400 mm, and 800 mm from this transducer back towards the diaphragm, to allow different combinations of measurements to be made.

7. CONCLUSIONS

The test results obtained and illustrated in Fig. 3 and Fig. 4 give high confidence that the pressure steps predicted by gas theory are realised in practice and that shock tube techniques can therefore be used to generate known inputs for the dynamic calibration of pressure transducers. An uncertainty budget for the step pressure generated within the plastic shock tube is given in Table 1, with estimated values of standard uncertainty given in italics in the fourth column. Making the assumption that the shock front is moving at constant velocity, it is apparent that the major sources of uncertainty for a pressure step of this magnitude are the distance and time measurements associated with the determination of this velocity. The other contributions could be reduced by various methods, such as using pure nitrogen rather than air as the driven gas, but the improvement to the final uncertainty would be minimal, when compared with a better measurement of the shock front velocity.

Table 1. Uncertainty budget for the plastic shock tube.

Parameter	Symbol	Value	Standard uncertainty	Unit	Sensitivity coefficient*	u^2
Adiabatic index	γ	1.401 0	*0.001 0*		1.2E+02	1.5E-02
Molar gas constant	R	8.314 462	0	J·mol^{-1}·K^{-1}	2.1E+01	0.0E+00
Temperature	T	293.15	*0.10*	K	5.9E-01	3.4E-03
Molar mass	M	28.966	*0.010*	g·mol^{-1}	-5.9E+00	3.5E-03
Speed of sound	c_1	**343.35**	**0.15**	**m·s^{-1}**		**2.2E-02**
Distance	d	400.00	*0.25*	mm	1.4E+00	1.2E-01
Time interval	Δt	719.20	*0.50*	µs	-7.7E-01	1.5E-01
Shock speed	v_S	**556.17**	**0.52**	**m·s^{-1}**		**2.7E-01**
Shock speed	v_S	556.17	0.52	m·s^{-1}	2.9E-03	2.3E-06
Speed of sound	c_1	343.35	0.15	m·s^{-1}	-4.7E-03	4.9E-07
Mach number	$\mathcal{M}$	**1.619 8**	**0.001 7**			**2.8E-06**
Driven pressure	p_1	101 309	*100*	Pa	6.2E-06	3.9E-07
Mach number	$\mathcal{M}$	1.619 8	0.001 7		1.6E+00	7.5E-06
Pressure step	Δp	**0.629 2**	**0.002 8**	**MPa**		**7.9E-06**
			0.45	**%**		

* The unit associated with the sensitivity coefficient is that of the quantity being calculated divided by the unit associated with the individual parameter, e.g. m·s^{-1}·K^{-1} for temperature T

It is hoped that the careful design and manufacture of the 7 MPa steel shock tube, together with precise measurements of time and distance to quantify shock wave velocity at the end-wall, will enable the end-wall pressure step to be determined with an expanded uncertainty (at $k = 2$) of better than 1 %.

ACKNOWLEDGMENTS

This work is supported by the UK's Department for Business, Innovation & Skills, under the National Measurement System's Engineering and Flow Metrology Programme, and has also received support from the European Metrology Research Programme (EMRP). The EMRP is jointly funded by the EMRP participating countries within EURAMET (the European Association of National Metrology Institutes) and the European Union. The authors would also like to thank Chris Neill of the University of Exeter who carried out parts of the practical work and data analysis.

REFERENCES

[1] S. Downes, A. Knott and I. Robinson, "Towards a shock tube method for the dynamic calibration of pressure sensors", *Phil. Trans. R. Soc. A*, 372: 20130299, July 2014.

[2] C. Matthews et al., "Mathematical modelling to support traceable dynamic calibration of pressure sensors", *Metrologia*, vol. 51, nº. 3, pp. 326-338, June 2014.

[3] H. Pain and E. Rogers, "Shock waves in gases," *Reports on progress in physics*, vol. 25, no. 1, pp. 287-336, 1962.

[4] D. Holder and D. Schultz, *On the Flow in a Reflected-Shock Tunnel*, HMSO, London, 1962.

[5] S. Downes, A. Knott and I. Robinson, "Determination of pressure transducer sensitivity to high frequency vibration", *IMEKO 22nd TC3, 12th TC5 and 3rd TC22 International Conferences*, Cape Town, South Africa, Feb. 2014.